

# Localized Character of $4f$ Electrons in $\text{CeRh}_x$ ( $x=2,3$ ) and $\text{CeNi}_x$ ( $x=2,5$ )

Ran-Ju Jung,<sup>1</sup> Byung-Hee Choi,<sup>1</sup> Hyeong-Do Kim,<sup>1</sup> S.-J. Oh,<sup>1,\*</sup> En-Jin Cho,<sup>2</sup> T. Iwasaki,<sup>3</sup> A. Sekiyama,<sup>3</sup> S. Imada,<sup>3</sup> S. Suga,<sup>3</sup> and J.-G. Park<sup>4</sup>

<sup>1</sup>*School of Physics & Center for Strongly Correlated Material Research, Seoul National University, Seoul 151-742, Korea*

<sup>2</sup>*Department of Physics, Chonnam National University, Kwangju 500-757, Korea*

<sup>3</sup>*Department of Material Physics, Osaka University, Osaka 560-8531, Japan*

<sup>4</sup>*Department of Physics, Sungkyunkwan University, Suwon 402-751, Korea*

We have measured Ce  $4f$  spectral weights of extremely  $\alpha$ -like Ce-transition metal intermetallic compounds  $\text{CeRh}_x$  ( $x=2,3$ ) and  $\text{CeNi}_x$  ( $x=2,5$ ) by using the *bulk-sensitive* resonant photoemission technique at the Ce  $M_5(3d_{5/2} \rightarrow 4f)$ -edge. Unprecedentedly high energy resolution and longer escape depth of photoemitted electron at this photon energy enabled us to distinguish the sharp Kondo resonance tails at the Fermi level, which can be well described by the Gunnarsson-Schönhammer(GS) calculation based on the Anderson Impurity Hamiltonian. On the other hand, the itinerant  $4f$  band description shows big discrepancies, which implies that Ce  $4f$  electrons retain localized characters even in extremely  $\alpha$ -like compounds.

PACS numbers: 79.60.-i, 71.20.Eh, 71.28.+d

Cerium is the first element of the  $4f$  rare-earth series in the periodic table, and occupies a special place in the condensed matter physics in that its  $4f$  electron is believed to lie on the borderline between localization and itinerancy. Its occupied  $4f$  orbital is more extended than those of heavier rare earths, and it is generally believed that an appropriate description of the interaction between the  $4f$  state and the conduction bands is essential to understand the physics of cerium metal and cerium-based compounds. The famous ' $\gamma$ - $\alpha$ ' phase transition in cerium metal is a case in point. This isostructural transition is associated with a large volume change ( $\approx 15\%$ ) and loss of magnetism, and although it has been investigated for more than 50 years the nature of phase transition still remains controversial. The early "promotional model"[1] where one Ce  $4f$  electron is presumed to go into the  $5d-6s$  conduction band in the  $\alpha$  phase was not supported by many experiments, and two other models based on quite different starting points have emerged.

One is the Mott transition model advocated by B. Johansson[2], which supposes that Ce  $4f$  electron is localized and non-bonding in the  $\gamma$  phase, but becomes itinerant and forms a  $4f$  band in the small volume  $\alpha$  phase. The recent calculation on the ground state properties of Ce metal based on the self-interaction corrected local (spin) density approximation (SIC-L(S)DA) seems to support this idea[3], and even the phase diagram has been calculated [4]. The other model is the Kondo volume collapse model[5, 6], which proposes that  $4f$  electron is localized in both  $\gamma$  and  $\alpha$  phases and the phase transition is caused by the change in the conduction electron screening of the  $4f$  electron. In this model the Anderson impurity hamiltonian is used to describe both spectroscopic and thermodynamic properties[7, 8], and the ' $\gamma$ - $\alpha$ ' phase transition was explained as due to the variation of hybridization strength between  $4f$  and conduction

states[5]. Hence quite distinct pictures on the electronic structure of  $\alpha$ -Ce have emerged from these two models.

These contrasting views on the nature of Ce  $4f$  electron, *i.e.* "localized" vs "itinerant", extend to the understanding of electronic structures of Ce compounds. For example, when cerium alloys with transition metal(TM) element to form intermetallic compounds, the hybridization between the  $4f$  state and the  $d$  state of TM can be much larger than the corresponding hybridization in Ce metal[9, 10]. In these so-called extremely  $\alpha$ -like Ce-TM compounds, it was suggested that the itinerant  $4f$  picture forming a narrow band is rather proper, and that this itinerant description makes correct predictions on the equilibrium lattice constant and magnetic moment in agreement with experiments for such compounds as  $\text{CeFe}_2$ ,  $\text{CeRh}_x$  ( $x=2,3$ ), and  $\text{CeNi}_x$  ( $x=2,5$ )[11, 12]. On the other hand, these compounds have also been analyzed within the Anderson impurity model[13].

Photoelectron spectroscopy directly probes the electronic structure (single-particle excitation spectrum in the many-body description) of solids, and can in principle distinguish between these two contrasting pictures. Indeed for  $\text{CeRh}_3$ , it was claimed that photoemission and inverse photoemission spectra are consistent with the  $4f$  band picture[10, 14]. But this interpretation was challenged later[15], while many other Ce-TM compound photoemission data had been successfully interpreted within the Anderson impurity model[13]. One important factor contributing to this controversy is the fact that most high-resolution photoemission experiments on Ce compounds so far have been performed with low energy photons ( $h\nu \leq 150$  eV), which makes the spectra quite surface-sensitive[16]. Since the coordination number becomes smaller at the surface, the hybridization of Ce  $4f$  states with TM  $d$  levels is reduced, favoring localized  $4f$  electron picture[17]. Therefore, to understand

the bulk electronic structures it is necessary to separate out the surface contribution from the bulk, but there are many uncertainties and ambiguities in this procedure[18]. Hence it is desirable to obtain *bulk-sensitive*  $4f$  spectra from direct experiments to resolve this controversy.

In this Letter, we report such study of the *bulk-sensitive*  $4f$  spectral weights in extremely  $\alpha$ -like Ce-TM intermetallic compounds  $\text{CeRh}_x$  ( $x=2,3$ ) and  $\text{CeNi}_x$  ( $x=2,5$ ), which are believed to be most likely to form itinerant  $4f$  band among Ce compounds. Such bulk-sensitive high-resolution photoemission experiments were made possible in a recently developed synchrotron radiation beamline[19], where high energy photons are incident to utilize the longer escape depth of the emitted photoelectrons. Since the photoionization cross section of Ce  $4f$  electron is usually much less than those of TM  $d$  electrons, we used the resonance photoemission (RPES) technique at the Ce  $3d$ -edge to obtain the partial  $4f$  spectral weights, where the  $4f$  emission is enhanced relative to other conduction electron emissions by the process

$$3d^{10}4f^1 + \hbar\omega \rightarrow 3d^94f^2 \rightarrow 3d^{10}4f^0 + \text{photoelectron}$$

Similar resonance photoemission technique has been extensively used at the Ce  $4d$ -edge to obtain  $4f$  spectral weights of many Ce compounds[13]. The difference between RPES at these two edges is that the kinetic energy of the valence photoelectron is  $\sim 880$  eV at the Ce  $3d$ -edge, whereas it is  $\sim 120$  eV at the  $4d$ -edge. Hence the escape depth of photoemitted electron at the  $M_5$ -edge is much longer than  $4d$  RPES, and the spectra becomes bulk sensitive with less than  $\sim 15\%$  of total weights contributing from the surface region[16]. This technique has proven to be effective in elucidating bulk electronic structures of several Ce compounds[20, 21].

All samples of  $\text{CeRh}_2$ ,  $\text{CeRh}_3$ ,  $\text{CeNi}_2$  and  $\text{CeNi}_5$  were polycrystalline made by argon arc-melting followed by annealing, and their crystal structures were checked by x-ray diffraction. The Ce  $3d \rightarrow 4f$  RPES and x-ray absorption spectroscopy (XAS) measurements at the Ce  $M_{4,5}$  edge were performed in the beamline BL25SU of SPring-8 in Japan. The energy resolution of the photon source around Ce  $M_{4,5}$  edge was better than 80 meV (Full width at half maximum : FWHM) and the overall experimental resolution  $\sim 100$  meV FWHM was obtained by SCIENTA SES200 electron analyzer. The pressure in the vacuum chamber was better than  $4 \times 10^{-10}$  Torr during the measurements. The data were taken at 20 K and temperature was controlled by closed-cycle He cryostat. Sample surfaces were cleaned by filing with a diamond file *in situ* and we checked the cleanliness of the surface by monitoring O  $1s$  level. The  $E_F$  of the sample was referred to that of surface-cleaned Pd metal.

Figure 1 shows the x-ray absorption spectra of  $\text{CeNi}_x$  ( $x=2,5$ ) at the Ce  $M_5$  edge corresponding to the transition  $3d_{5/2} \rightarrow 4f$ . The lineshape of the main peak

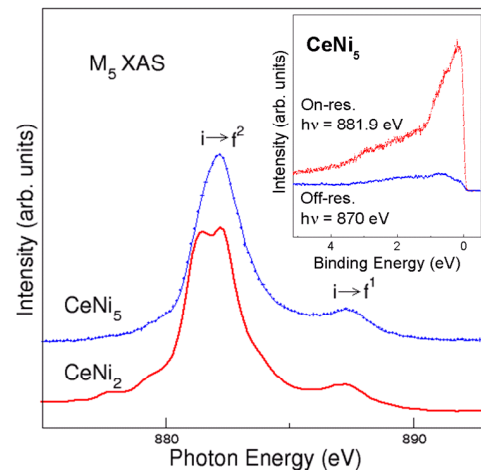


FIG. 1: The Ce  $M_5$  XAS spectra of  $\text{CeNi}_x$  ( $x=2,5$ ). The inset shows off- and on-resonance photoemission data on  $\text{CeNi}_5$ .

structure near  $h\nu = 882.3$  eV is primarily determined by the multiplet structures of the  $\underline{3d}f^2$  electronic configuration, where the underline represents a hole[22]. The slight change of this lineshape and the satellite structure near  $\sim 885$  eV can be understood as the effect of hybridization between Ce  $4f$  electron and the valence band within Anderson impurity model [23, 24]. In the inset, we show the photoemission spectra of  $\text{CeNi}_5$  taken at photon energy below this edge ( $h\nu = 870$  eV; off-resonance) and very close to the maximum ( $h\nu = 881.9$  eV; on-resonance). We can see the drastic change of spectral shapes due to the much enhanced Ce  $4f$  emissions on resonance. We then extract the *bulk-sensitive*  $4f$  spectral weights of each compound by subtracting off-resonance data from the on-resonance data. In this process, we use the on-resonance spectra at slightly lower ( $\sim 0.4$  eV) incident photon energy than the  $M_5$  maximum peak of XAS, since the spectra taken at the  $M_5$  maximum peak position are often found to be contaminated by incoherent Auger emissions[25].

The experimental bulk-sensitive  $4f$  spectral weights of  $\text{CeNi}_2$  and  $\text{CeNi}_5$  thus obtained are shown as black dots in Figure 2. Previously reported high resolution ( $\Delta E \sim 50$  meV)  $4d \rightarrow 4f$  resonant photoemission[28] observed the  $4f$ -driven spectral feature less clear due to the dominant TM  $3d$  emission. However, present work evidently shows the  $4f$ -driven peak at the Fermi level in both Ce-Ni compounds. To determine whether “localized” or “itinerant” picture is more appropriate for these  $4f$  spectral weights, we plot and compare with both the Ce  $4f$  density-of-states (DOS) from linear muffin-tin orbital (LMTO) calculations with local density approximation (thin solid line)[10], and the Gunnarsson Schönhammer (GS) calculation fit (thick solid line) based on the Anderson single impurity model[7]. The one-electron  $4f$  DOS were taken from the published band structure calculations[10], which were convoluted with

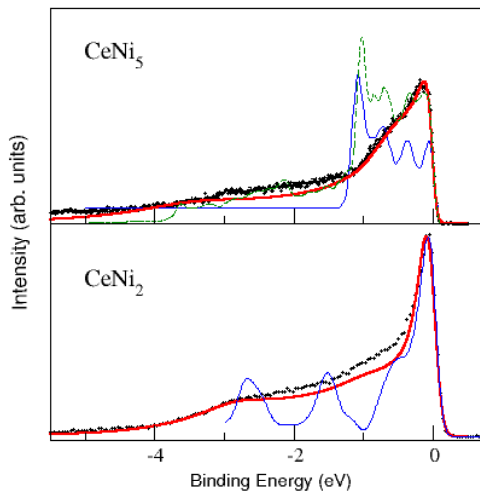


FIG. 2: Comparison between the experimental Ce 4*f* spectral weights (dots) with band structure calculations (thin solid line) and with GS fits (thick solid line) for CeNi<sub>*x*</sub> (*x* = 2, 5). The dashed line in the top panel is another band calculation by Harima [29].

TABLE I: The parameter values used for GS fitting and the resulting 4*f*-level occupancy number *n<sub>f</sub>* and the Kondo temperature *T<sub>K</sub>*. Coulomb energy *U<sub>ff</sub>* is set to 6.0 eV.  $\chi_m(0)$ 's are magnetic susceptibility at *T*=0 predicted from GS fitting and  $\chi_m^*(0)$ 's are experimental values in units of  $10^{-3}emu/mol$ .

	$\varepsilon_f$ (eV)	$\Delta$ (meV)	<i>T<sub>K</sub></i> (K)	<i>n<sub>f</sub></i>	$\chi_m(0)$	$\chi_m^*(0)$
CeRh <sub>2</sub>	1.30	95	1335	0.76	0.92	0.6
CeRh <sub>3</sub>	1.20	110	1350	0.70	0.54	0.4
CeNi <sub>2</sub>	1.13	89	570	0.78	1.13	0.9
CeNi <sub>5</sub>	1.00	90	3300	0.69	0.62	0.7

Lorentzian broadening in the form of  $\alpha|\omega - \omega_0|$  and the experimental resolution of 100 meV. For the GS calculations the lowest order *f*<sup>0</sup>, *f*<sup>1</sup>, *f*<sup>2</sup>, and the second-order *f*<sup>0</sup> states are employed as basis states, and the spin-orbit splitting of the 4*f* level is included. When GS calculation is executed, it is known to be quite essential to employ realistic *V*<sup>2</sup>( $\epsilon$ ) in order to fully interpret experimental spectra and fit the thermodynamic quantities [26]. Hence we used the 3*d* → 4*f* off-resonance spectrum for the valence band shape to be hybridized with Ce 4*f* state.

From these comparisons, we can see that the GS calculations provide quite good fits for the experimental Ce 4*f* spectral weights for both CeNi<sub>2</sub> and CeNi<sub>5</sub>. Their resulting parameter values are presented in Table I along with the Kondo temperature *T<sub>K</sub>*, the 4*f* electron occupation number *n<sub>f</sub>*, the magnetic susceptibilities at *T* = 0,  $\chi_m(0)$  deduced from these parameter values and the experimentally measured  $\chi_m^*(0)$  [27]. We find that *T<sub>K</sub>* increases and *n<sub>f</sub>* becomes smaller as the Ni content is increased, which is consistent with the findings of XAS and other

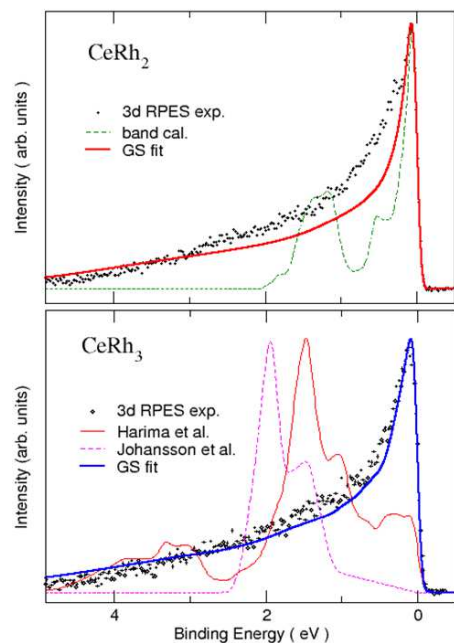


FIG. 3: The comparisons of experimentally extracted *bulk-sensitive* 4*f* weights of CeRh<sub>2</sub> and CeRh<sub>3</sub> with the one-electron band calculations and the GS fit.

spectroscopic investigations[23], and can be attributed to the shift of the Ni 3*d* valence band toward to the Fermi level at high Ni concentration[28]. We also find that the  $\chi_m(0)$  deduced from GS calculation gives very close values to measured ones for both Ce-Ni compounds.

On the other hand, the band structure calculation gives rather poor agreement with the experimental data for both compounds, especially in CeNi<sub>5</sub>. The calculation does not reproduce the peak near the Fermi level properly, and the predicted strongest peak around 1 eV from the Fermi level is absent in the experimental data. This discrepancy is not due to the particular calculation method or misplacement of the Fermi level, since more recent band calculation from other group (dot-dashed line in the figure) also shows similar discrepancy[29]. For the cases of CeNi<sub>2</sub>, the band calculations reproduce the peak at the Fermi level properly, but the features between 1-3 eV from the Fermi level shows appreciable discrepancy. These disagreements of band descriptions imply that the correlation between the 4*f* electrons should not be neglected in these CeNi compounds, even in the extremely  $\alpha$ -like compound CeNi<sub>5</sub>.

The same phenomena happen in CeRh<sub>*x*</sub> (*x*=2,3) compounds, as can be seen in Figure 3. In this figure, the experimental bulk-sensitive 4*f* spectral weights [30] (dots) are compared with the one-electron band structure calculation (thin solid line) and the fit of the GS calculation (thick solid line). In both CeRh<sub>2</sub> and CeRh<sub>3</sub> the experimental data show a large peak near the Fermi level reminiscent of the Kondo tail, which can be well described by

the GS calculation. However, the band structure calculations done by two independent groups[10, 29] completely miss this feature in CeRh<sub>3</sub>, and predict instead a strong peak near 2 eV from  $E_F$ , which is absent in the experimental data. Even in the case of CeRh<sub>2</sub>, the band structure correctly predicts a peak near  $E_F$ , but again DOS below 2 eV from  $E_F$  shows substantial disagreement. On the other hand, GS calculations give good general agreement in both Ce-Rh compounds, although some discrepancy in intensity around 1 eV from  $E_F$  is seen in CeRh<sub>2</sub>. Such disagreement seems to be commonly observed in Laves-phase CeTM<sub>2</sub> compounds[24], and its origin is unknown at present. We list the parameter values of GS fitting for CeRh<sub>2</sub> and CeRh<sub>3</sub> in Table I along with their  $T_K$ ,  $n_f$ ,  $\chi_m(0)$  and  $\chi_m^*(0)$ . We find that  $\chi_m(0)$  is in good agreement with  $\chi_m^*(0)$  in both Ce-Rh compounds as in Ce-Ni case.

It may not be surprising that the band calculation does rather poorly in describing photoemission spectra although it can correctly predict volume anomaly and magnetic moment, since the local density approximation is strictly valid only for the ground state. However many physical properties such as specific heat depend on the excitation spectrum, and the fact that itinerant  $4f$  band picture fails to describe the single-particle excitation such as photoemission implies that it will not be able to understand many physical properties of the system. On the other hand, Anderson impurity model gives consistent description of both  $4f$  spectral weights and thermodynamic properties with one set of parameter values, as seen above in Figs. 2-3 and Table I. This shows that electron correlation effect is important even for these extremely  $\alpha$ -like Ce compounds, and that the localized  $4f$  picture may be a better starting point than the itinerant band picture to understand their physical properties.

In summary, the *bulk-sensitive* Ce  $4f$  spectral weights obtained by  $3d \rightarrow 4f$  RPES of CeNi<sub>x</sub> ( $x=2, 5$ ) and CeRh<sub>x</sub> ( $x=2, 3$ ) show remarkably enhanced the  $f^1$  final state peak near the Fermi level unlike those of  $4d \rightarrow 4f$  RPES. The Gunnarsson Schönhammer calculations based on the Anderson single impurity model fit very well the experimental Ce  $4f$  spectral weights, and its resulting parameter values are consistent with other spectroscopic and thermodynamic data. However, one-electron band calculations fail to give plausible descriptions. This implies that the  $4f$  states even in extremely  $\alpha$ -like CeRh<sub>2</sub>, CeRh<sub>3</sub>, and CeNi<sub>5</sub> still retain ‘localized’  $4f$  character, at least for the excitation spectra.

This work is supported by the Korean Science and Engineering Foundation through the Center for Strongly Correlated Materials Research at Seoul National University. The experiments were performed under the approval of the Japan Synchrotron Radiation Research Institute. We thank Prof. Harima for sending band calculation results prior to publication.

- [1] W.H.Zachariasen (unpublished) quoted in A.W. Lawson and T.Y. Tang, Phys. Rev. **76**, 301 (1949); L. Pauling, J. Am. Chem. Soc. **69**, 542 (1947).
- [2] B. Johansson, Philos. Mag. **30**, 469 (1974).
- [3] Z. Szotek *et al.*, Phys. Rev. Lett. **72**, 1244 (1994); A. Svane, Phys. Rev. Lett. **72**, 1248 (1994).
- [4] B. Johansson *et al.*, Phys. Rev. Lett. **74**, 2335 (1995); T. Jarlborg *et al.*, Phys. Rev. B **55**, 1288 (1997).
- [5] J. W. Allen and R. M. Martin, Phys. Rev. Lett **49**, 1106 (1982); L. Z. Liu *et al.*, Phys. Rev. B **45**, 8934 (1992); J. W. Allen and L. Z. Liu, Phys. Rev. B **46**, 5047 (1992).
- [6] M. Lavagna, C. Lacroix, and M. Cyrot, Phys. Lett. **90A**, 210 (1982); J. Phys. F **13**, 1007 (1983).
- [7] O. Gunnarsson and K. Schönhammer, Phys. Rev. Lett. **50**, 604 (1983); Phys. Rev. B **28**, 4315 (1983).
- [8] F. Patthey *et al.*, Phys. Rev. B **42**, 8864 (1990).
- [9] L. Nordström and B. Johansson, Phys. Rev. B **44**, 10031 (1991).
- [10] L. Severin and B. Johansson, Phys. Rev. B **50**, 17886 (1994).
- [11] O. Eriksson *et al.*, Phys. Rev. Lett. **60**, 2523 (1988); J. Trygg *et al.*, Phys. Rev. B **50**, 4200, (1994).
- [12] Lars Nordström *et al.*, Phys. Rev. B **46**, 3458 (1992).
- [13] J. W. Allen, S.-J. Oh, O. Gunnarsson, K. Schönhammer, M. B. Maple, M. S. Torikachvili, and I. Lindau, Adv. Phys. **35**, 275 (1986) and references therein.
- [14] E. Weschke *et al.*, Phys. Rev. Lett. **69**, 1792 (1992).
- [15] D. Malterre *et al.*, Phys. Rev. Lett. **73**, 2005 (1994); D. Malterre *et al.*, Adv. Phys. **45**, 299 (1996).
- [16] Stefan Hüfner, “Photoelectron Spectroscopy”, (Springer-Verlag, Berlin, 1995) p.8.
- [17] L. Duò, Surf. Sci. Rep. **32**, 233 (1998).
- [18] Hyeong-Do Kim *et al.*, Phys. Rev. B **59**, 12294 (1999).
- [19] Y. Saitoh *et al.*, J. Synchrotron Rad. **5**, 542 (1998).
- [20] A. Sekiyama *et al.*, Nature **403**, 396 (2000); J. Phys. Soc. Jpn. **69**, 2771 (2000); Solid State Commun. **121**, 561 (2002).
- [21] T. Iwasaki *et al.*, Phys. Rev. B **65**, 195109 (2002).
- [22] T. Jo, and A. Kotani, Phys. Rev. B **38**, 830 (1988).
- [23] J.C. Fuggle *et al.*, Phys. Rev. B **27**, 4637 (1983).
- [24] Ran-Ju Jung, Ph.D thesis, Seoul National University, Korea (2001).
- [25] E.-J. Cho *et al.*, submitted to Phys. Rev. B.
- [26] See-Hun Yang *et al.*, Phys. Rev. B **61**, R13329 (2000).
- [27] For CeRh<sub>2</sub> M. Ozawa *et al.*, Physica B **206 & 207**, 267 (1995); for CeRh<sub>3</sub> T. Gambke *et al.*, “Valence Fluctuations in Solid”,(North-Holland, Amsterdam, 1981) p.447; for CeNi<sub>2</sub> J. Sakurai *et al.*, J. Magn. Mater. **52**, 205 (1985); for CeNi<sub>5</sub> D. Gignoux *et al.*, J. de Phys. **43**, 173 (1982). Whenever possible, the susceptibility of the corresponding Y or La compound was subtracted to obtain the contribution from Ce ions only.
- [28] D. Purdie *et al.*, Solid State Commun. **106**, 799 (1998).
- [29] H. Harima, private communications.
- [30] Our 3d RPES data on CeRh<sub>3</sub> is somewhat different from the old data[14] in that the peak at the Fermi level is much stronger and quite narrow. This is probably due to the difference in energy resolution and the incident photon energy.

---

\* Author to whom all correspondences should be addressed. e-mail: sjoh@plaza.snu.ac.kr